Supporting Information

Synthesis and characterization of rhodamine derivative as a selective switch-on fluorescent sensor for Cu^{2+} in aqueous PBS buffer and living cells

Maheshkumar Prajapati[a],Nidhi Pandey[b], Sarita Kalla[c], Sateesh Bandaru*[d] and Areti Sivaiah[a]*

Corresponding author: Dr. Areti Sivaiah* - Department of Chemistry, Sardar Vallabhai National Institute of Technology Surat, Surat-Dumas road, Surat-395007, Gujarat, India; Orcid.org/0000-0002-0388-3588; E-mail: areti@chem.svnit.ac.in

Sr.No.	Table of content	Page No.
S1	Synthesis and characterization of **P_2**	3
S2	Synthesis and characterization of **L_1**	5
S3	Synthesis and characterization of {**L_1**+Cu^{2+}} Complex	7
S4	Absorption titration **L_1** with of various metals ions	8
S5	Association constant obtained from the absorption titration of {L_1+Cu^{2+}} complex	9
S6	Job's plot obtained from the absorption titration	9
S7	Determination of Limit of Detection (LOD) of Cu^{2+} by **L_1**	9
S8	Comparison of the detection limits of recently developed fluorescent probes for Cu^{2+} in the literature.	10
S9	Competitive metal ion titration of **L_1** with Cu^{2+} in presence of other metal ions.	11
S10	Effect of pH on the fluorescence emission of **L_1** with Cu^{2+}.	11
S11	MTT assay of probe **L_1**	12
S12	Confocal fluorescence microscopy images study of **L_1** in presence of Cu^{2+} in HeLa cells.	12

S1. Synthesis and characterization of P_2

P_1 (1.0 g, 1.0 mmol) was accurately weighed and placed in glass round-bottom flask, and 60.0 mL of ethanol was added to fully dissolve it. After cooling at room temperature and adding 4.0 mL (70.0 mmol) of hydrazine hydrate solution (85.0%), the mixture was magnetically stirred and refluxed until the colour of **P_1** disappeared. The reaction solution was gradually cooled to room temperature, filtered under reduced pressure, and washed three times with ethyl alcohol to obtain the white solid product (**P_2**) in 65% yield (0.511 g).**FTIR (ATR, cm^{-1}):** 3430, 3343, 2948, 2866, 1687, 1613, 1510, 1200, 1150, 1003, 820, 739.**^{1}H NMR (600 MHz, $CDCl_3$) δ(ppm):**7.95(d, J = 4.88 Hz, 1H), 7.44(m, 2H), 7.05(d, J = 4.57 Hz, 1H), 6.38(s, 2H), 6.25(s, 2H), 3.57(s, 2H), 3.52(s, 2H), 3.21(dd, J = 7.14; 6.31 Hz, 4H), 1.90(s, 6H), 1.31(t, J = 7.08 Hz, 6H); **^{13}C NMR (150 MHz, $CDCl_3$) δ(ppm):**166.21, 152.25, 151.76,147.54, 132.58, 129.87, 128.13, 127.69, 123.81, 123.03, 117.99, 104.94, 96.85, 66.05, 38.36, 16.70, 14.75.

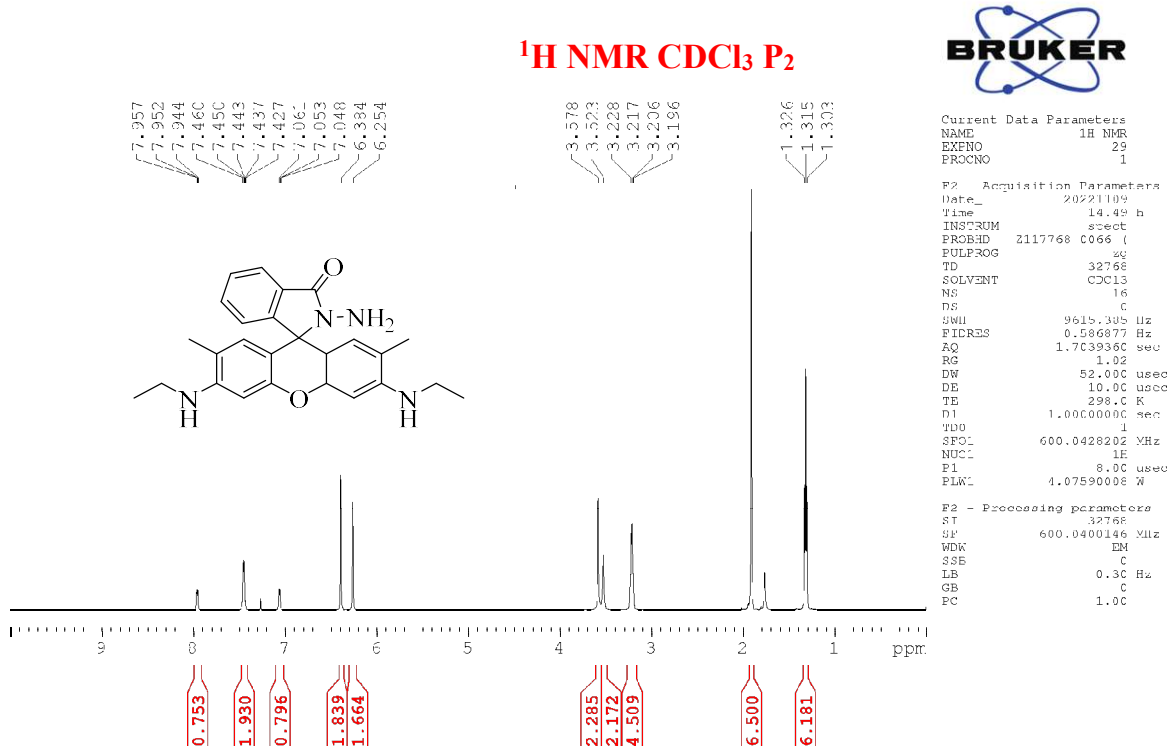

Fig.S1.^{1}H NMR spectrum of **P_2** in $CDCl_3$

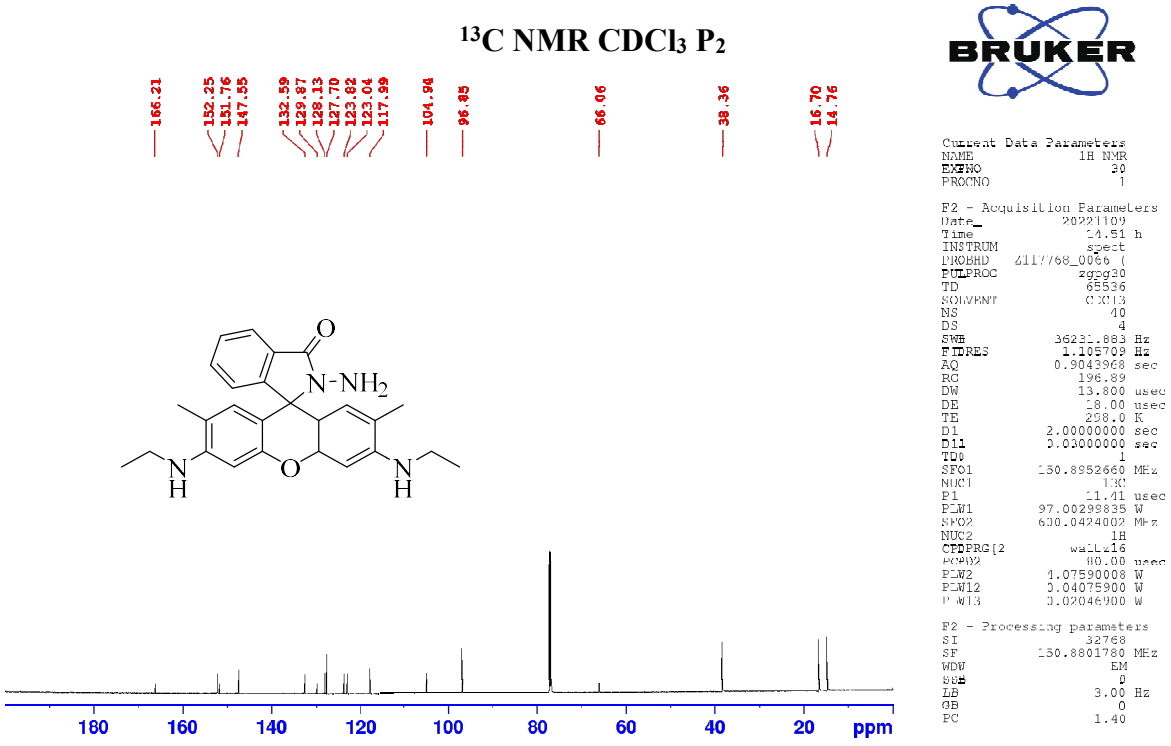

Fig.S1.^{13}C NMR spectrum of **P_2** in $CDCl_3$

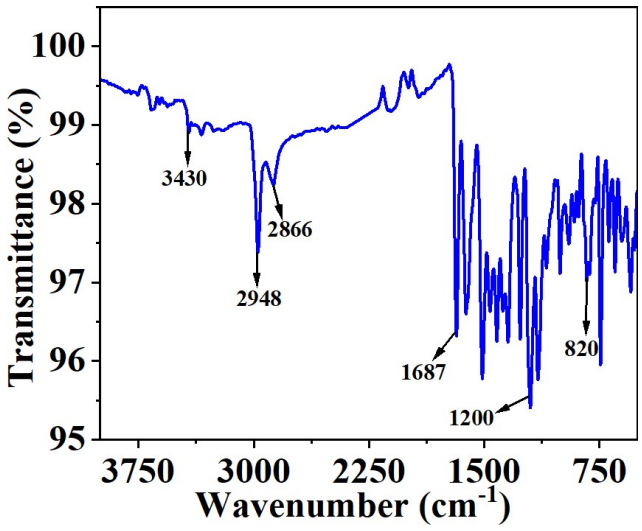

Fig.S1. FT-IR spectra of **P_2**

S2. Characterization of L_1

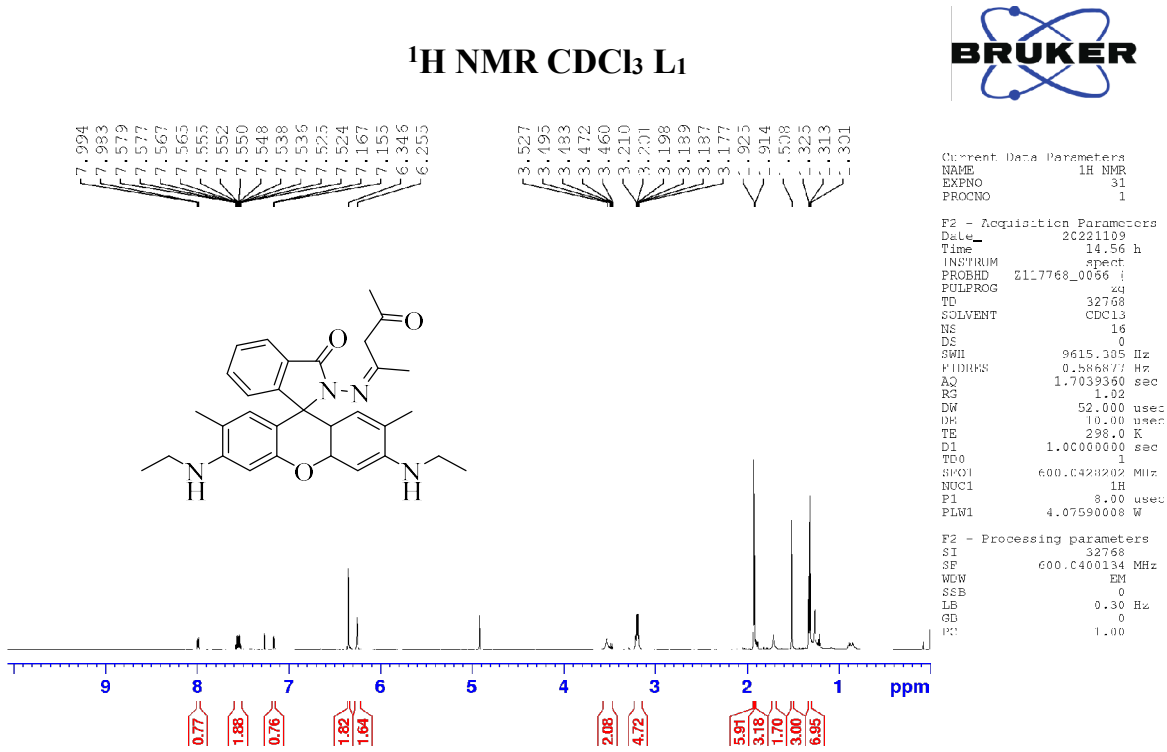

Fig.S2. ^{1}H NMR spectrum of Ligand (L_1) in $CDCl_3$

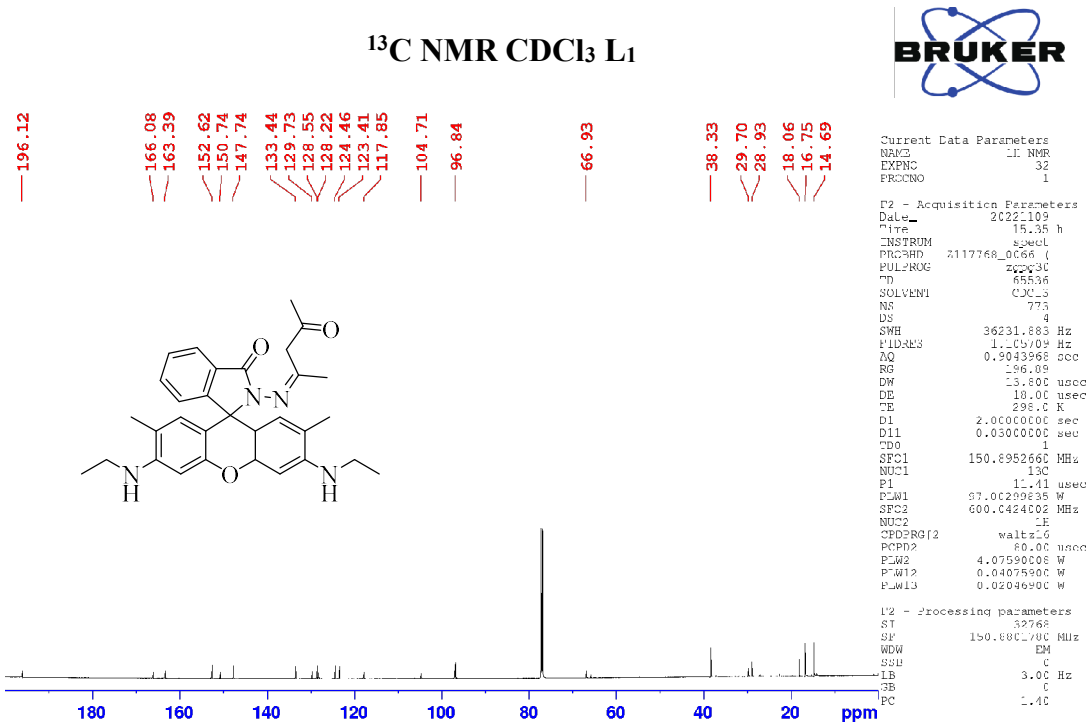

Fig.S2. ^{13}C-NMR spectrum of Ligand **(L_1)** in $CDCl_3$

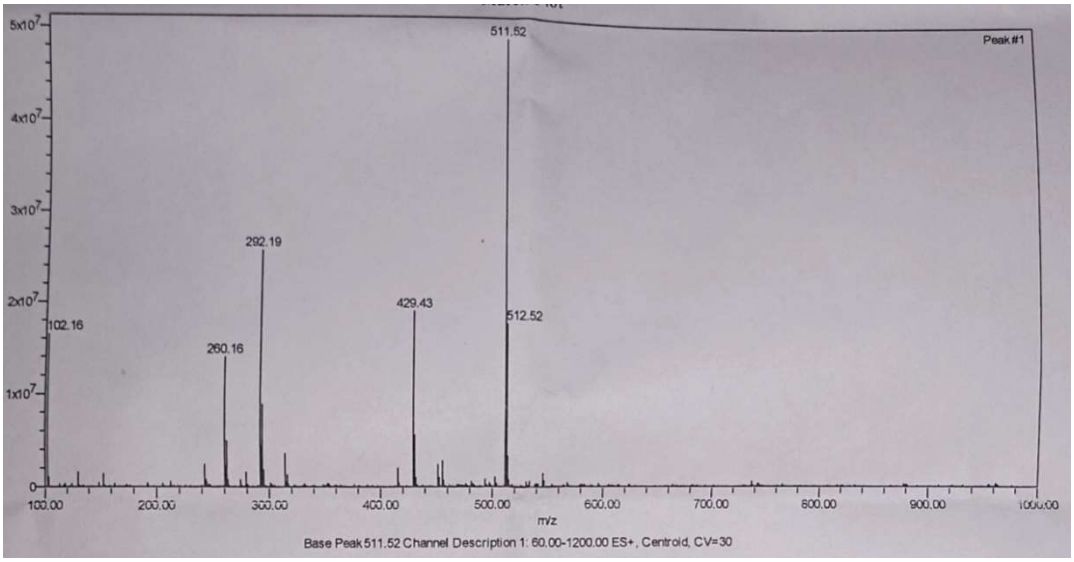

Fig. S2. Mass Spectra of Ligand $\mathbf{L_1}$: Calculated: 510.64; Observed: 511.52 $[M+H]^+$.

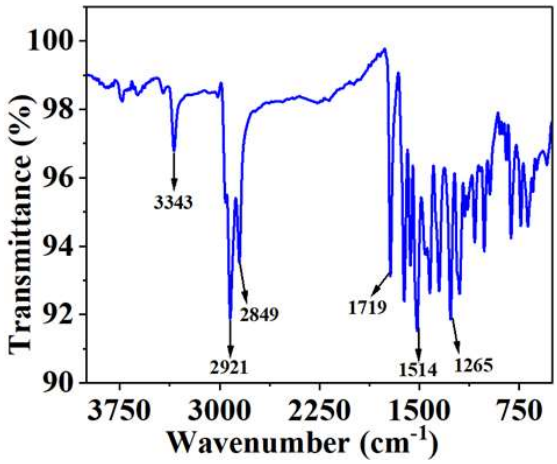

Fig.S2. FT-IR spectra of $\mathbf{L_1}$.

S3. Characterization of $\{L_1+Cu^{2+}\}$ complex

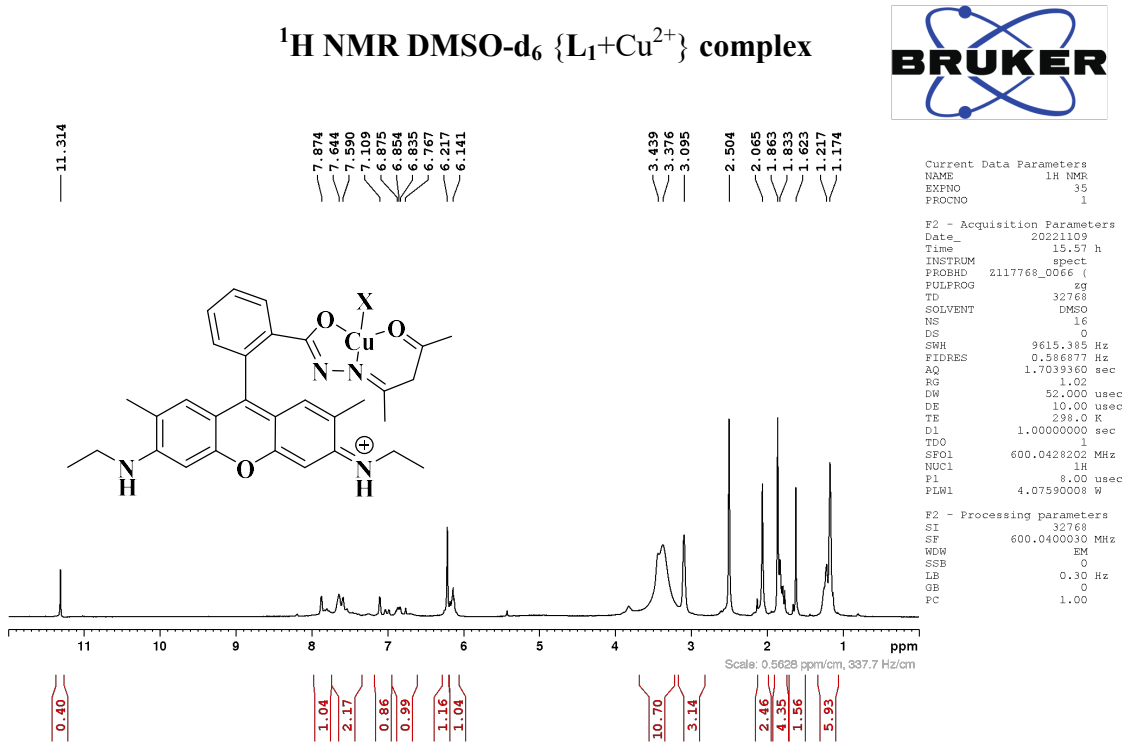

Fig.S3. ^{1}H NMR spectrum of $\{L_1+Cu^{2+}\}$ complex in DMSO-d$_6$

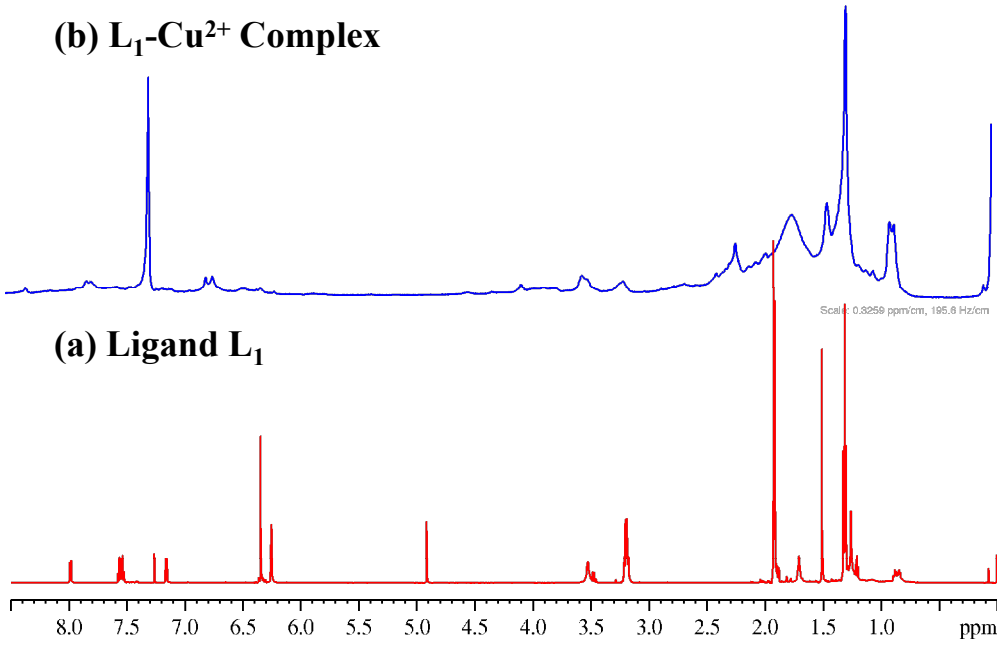

Fig. S3. Overlay ^{1}H-NMR spectra of (a) Ligand **(L_1)** (b) $\{L_1+Cu^{2+}\}$ Complex.

S4. Absorption titration L_1 with of various metals ions

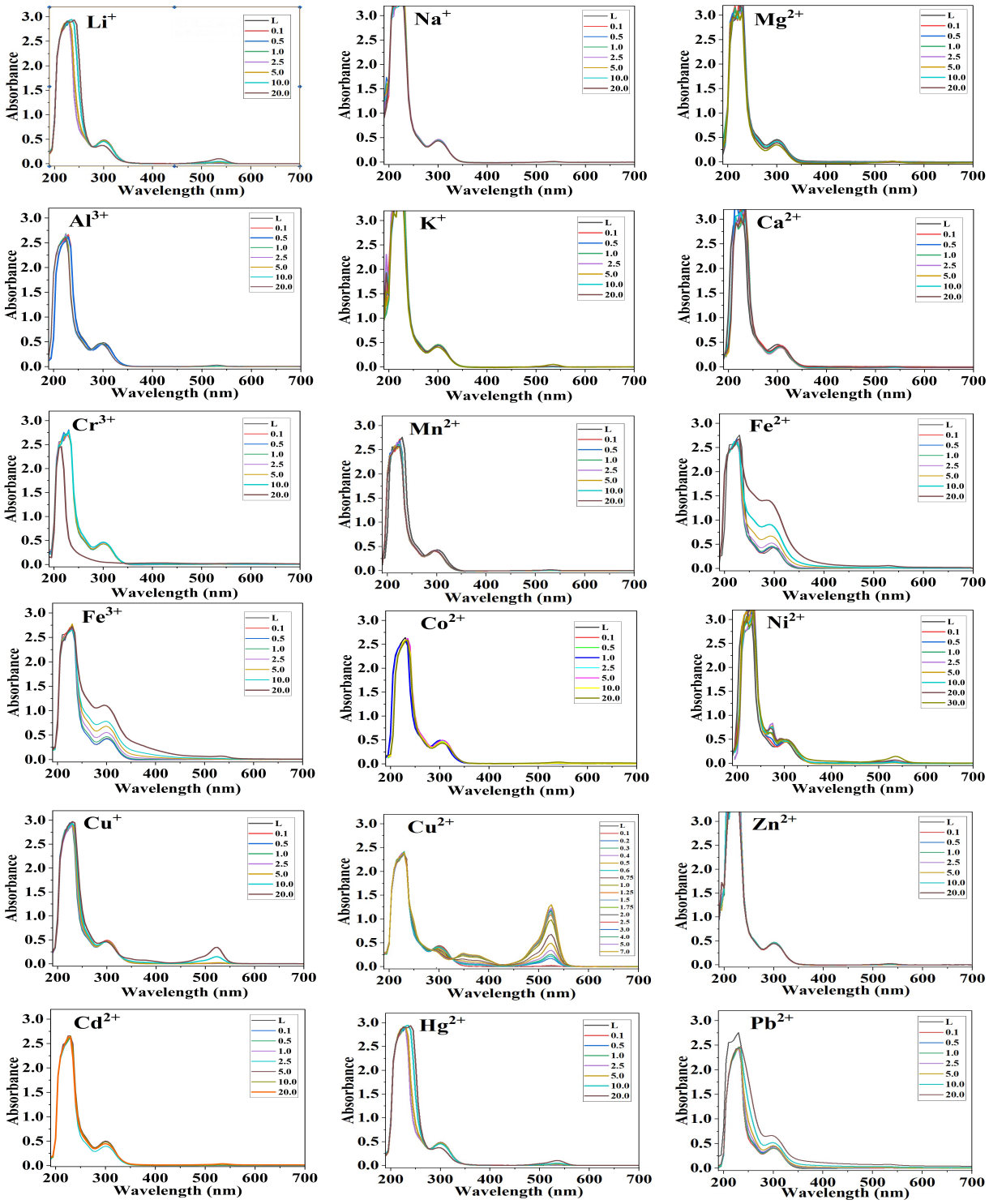

Fig.S4. Shows the absorbance spectra of $\mathbf{L_1}$ (10 μM) titrated with (0-20 eq.) of various concentrations of metals in ACN/PBS buffer (0.1 mM, pH 7.4, 1:1 of v/v).

S5. Association constant obtained from the absorption titration of {L_1+Cu^{2+}} complex

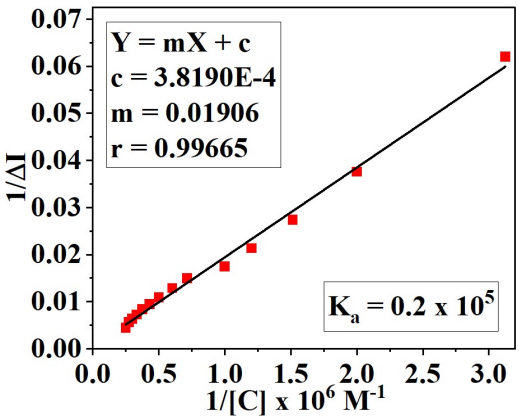

Fig.S5. Binding constant (K_a) of Ligand (L_1) with Cu^{2+}concentration in ACN: PBS (0.1 mM, pH = 7.4,v/v 1:1).

S6. Job's plot obtained from the absorption titration

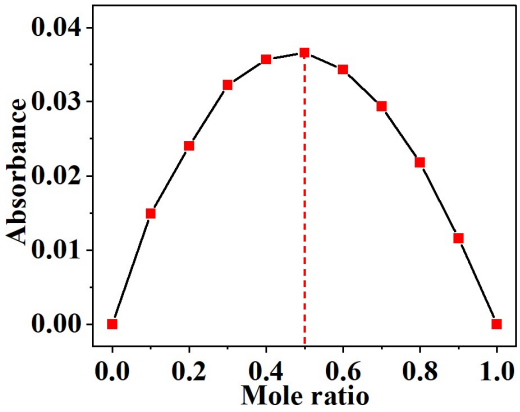

Fig.S6. Titration curve of L_1 and Cu^{2+} at constant concentration 20 mM in ACN: PBS solution (0.1 mM, pH= 7.4, 1:1 v/v).

S7. Determination of Limit of Detection (LOD) of Cu^{2+} by L_1

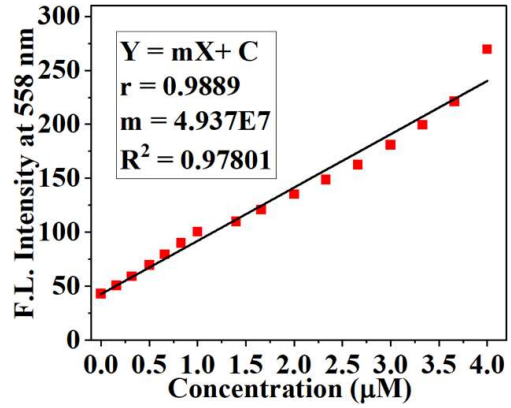

Fig.S7. Linear fluorescence relationship of Ligand (L_1) with Cu^{2+} (0-4μM) concentration in ACN: PBS (0.1 mM, pH = 7.4,v/v 1:1) at λ_{em} = 558 nm.

Table S8. Comparison of the detection limits of recently developed fluorescent probes for Cu^{2+} in the literature.

Sr. No.	Compound	Analytes	Solvent System	LOD	Application	Ref.
1	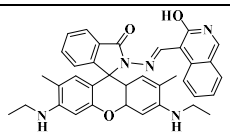	Cu^{2+}, Fe^{3+}	Aqueous medium	1.8 x 10^{-8} M	Trace out Fe^{3+}in zebrafish	**1**
2	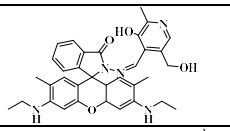	Cu^{2+}	Tris-HCl buffer	3.9 x 10^{-7} M	Lake water, drinking water	**2**
3	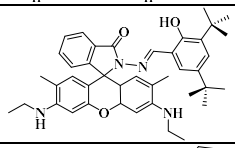	Cu^{2+}	ACN: H_2O	5.2 × 10^{-7} M	toxicity in Alzheimer disease	**3**
4	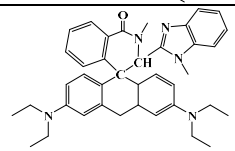	Cu^{2+}, S^{2-}	ACN: H_2O Tris HCl buffer, pH= 6.5	5.54 x 10^{-7} M	HeLa cells	**4**
5	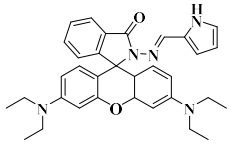	Cu^{2+}	ACN: HEPES buffer (pH 7.0, 1:1 of v/v)	28 x 10^{-8} M	Drinking water, Human serum, HeLa cells	**5**
6	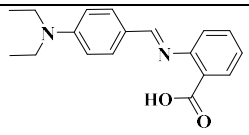	Cu^{2+},Fe^{2+}, Fe^{3+}	DMF	2.48 x 10^{-6} M	**NA**	**6**
7	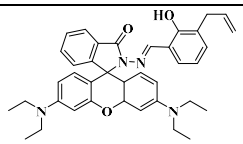	Cu^{2+}, Al^{3+}	H_2O:ACN (3:7, v/v, HEPES buffer, pH 7.4)	321 nM	Cell imagine studies in SiHa cells	**7**
8	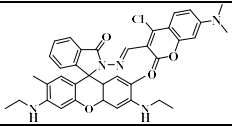	Hg^{2+}, Cu^{2+}	DMF: H_2O (2:8, v/v)	1.91 x 10^{-7} M	On filter paper and in water	**8**
9	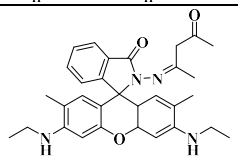	Cu^{2+}	ACN: PBS solution (0.1 mM, pH: 7.4, v/v =1:1)	3.58 x 10^{-8} M	L929 and HeLa cells	**Present work**

S09. Competitive metal ion titration of L_1 with Cu^{2+} in presence of other metal ions.

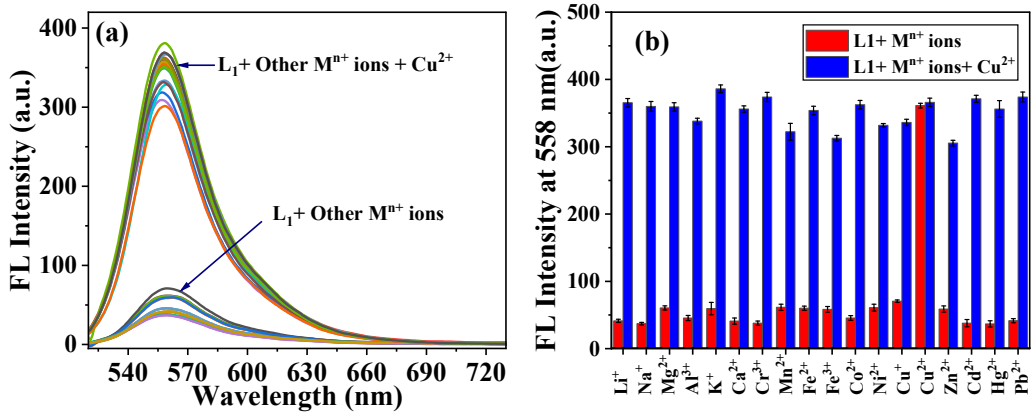

Fig.S09. Spectra from fluorescence titration of $\mathbf{L_1}$ (10 μM) with metal ions (100 μM) and (b) Histograms showing the fluorescence emission intensity at 558 nm of $\mathbf{L_1}$ with Cu^{2+} in the presence of competitive metal ions.

S10. Effect of pH on the fluorescence emission of L_1 with Cu^{2+}.

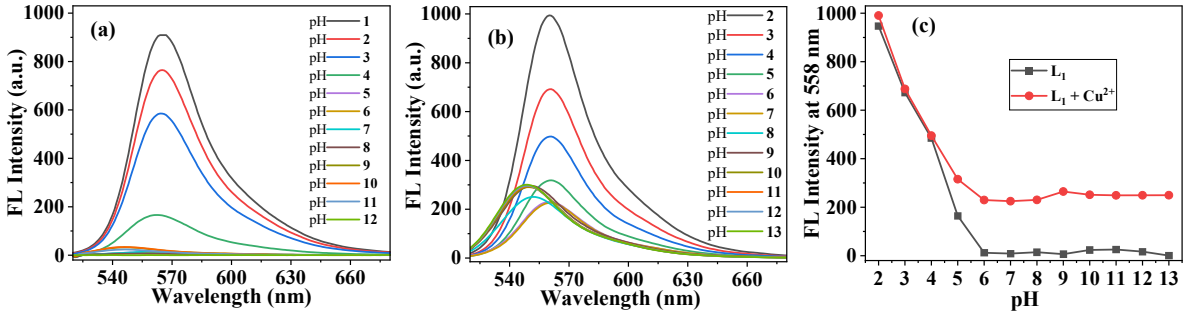

Fig. S10 Fluorescence response of (a) $\mathbf{L_1}$(10 mM), (b) {$\mathbf{L_1}$+Cu^{2+}} (10 eq.) and (c) corresponding fluorescence emission at 558 nm *vs*. pH range from 2 to 13.

S11. MTT assay of probe L_1

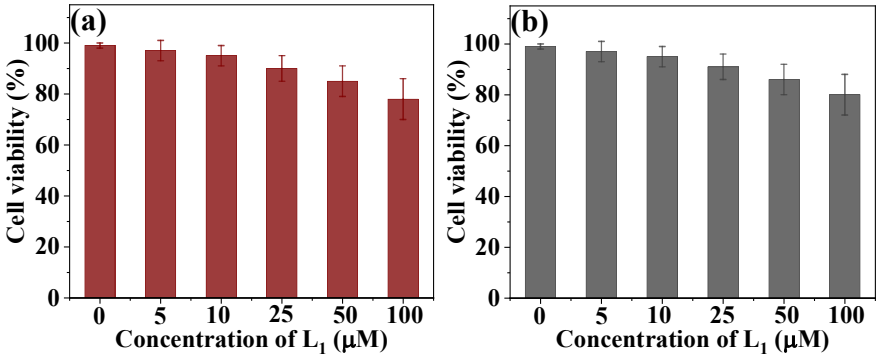

Fig. S11. MTT assay of probe $\mathbf{L_1}$ (a) L929 cells and (b) HeLa cells treated with different concentrations of probe $\mathbf{L_1}$ for 24 h.

S12. Confocal fluorescence microscopy images study of L_1 in presence of Cu^{2+} in HeLa cells.

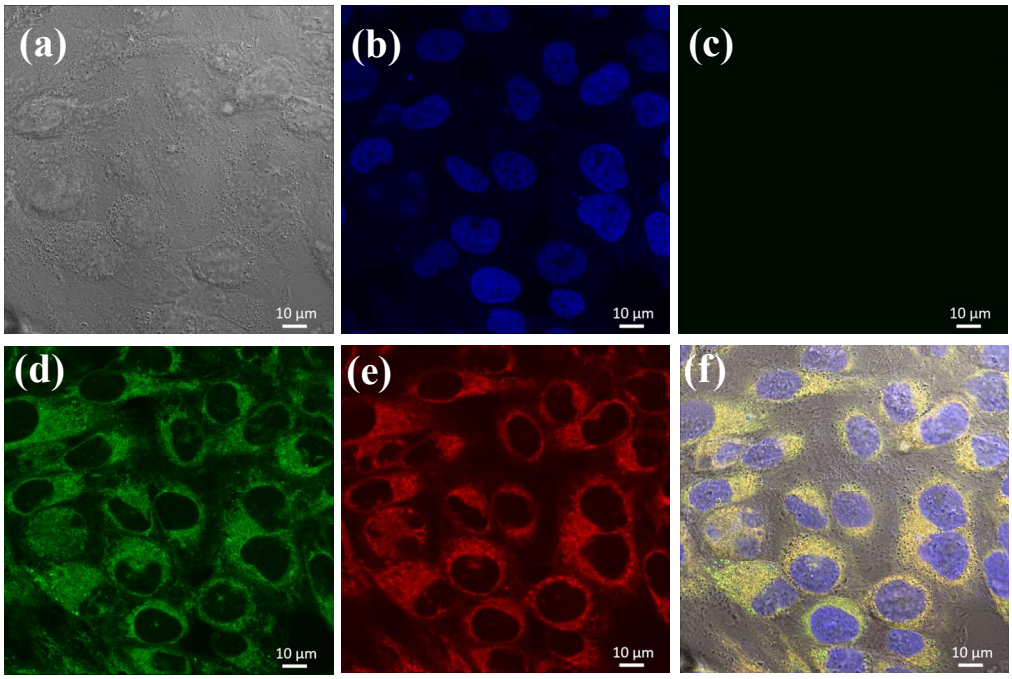

Fig. S12: Confocal fluorescence microscopy images were obtained from HeLa cells (a) DIC image, (c) cells were incubated only with $\mathbf{L_1}$ (10 μM), (d) cells treated with $\mathbf{L_1}$ followed by Cu^{2+} (20 μM) green Chanel and (e) red Chanel and (f) merged image of b, d and e.

References

1 A. S. Murugan, N. Vidhyalakshmi, U. Ramesh and J. Annaraj, Sensors and Actuators B : Chemical In vivo bio-imaging studies of highly selective , sensitive rhodamine based fl uorescent chemosensor for the detection of Cu 2+ / Fe 3+ ions, *Sensors Actuators B. Chem.*, 2018, **274**, 22–29.

2 Q. Huang, Y. T. Chen, Y. W. Ren, Z. Y. Wang, Y. X. Zhu and Y. Zhang, A rapid and naked-eye visible rhodamine 6G-based chemosensor for sensitive detection of copper(ii) ions in aqueous solution, *Anal. Methods*, 2018, **10**, 5731–5737.

3 B. S. Chauhan, A. Rai, A. K. Sonkar, K. Tripathi, S. Upadhyay, L. Mishra and S. Srikrishna, Neuroprotective Activity of a Novel Synthetic Rhodamine-Based Hydrazone against Cu^{2+}-Induced Alzheimer's Disease in Drosophila, *ACS Chem. Neurosci.,*2022, **13,** 1566-1579.

4 A. Majumdar, C. S. Lim, H. M. Kim and K. Ghosh, New Six-Membered pH-Insensitive Rhodamine Spirocycle in Selective Sensing of Cu2+ through C-C Bond Cleavage and Its Application in Cell Imaging, *ACS Omega*, 2017, **2**, 8167–8176.

5 P. Puangploy, S. Smanmoo and W. Surareungchai, A new rhodamine derivative-based chemosensor for highly selective and sensitive determination of Cu2+, *Sensors Actuators, B Chem.*, 2014, **193**, 679–686.

6 X. Zhu, Y. Duan, P. Li, H. Fan, T. Han and X. Huang, A highly selective and instantaneously responsive Schiff base fluorescent sensor for the 'turn-off' detection of iron(III), iron(II), and copper(II) ions, *Anal. Methods*, 2019, **11**, 642–647.

7 A. Rai, A. K. Singh, K. Tripathi, A. K. Sonkar, B. S. Chauhan, S. Srikrishna, T. D. James and L. Mishra, A quick and selective rhodamine based "smart probe" for "signal-on" optical detection of Cu2+ and Al3+ in water, cell imaging, computational studies and solid state analysis, *Sensors Actuators, B Chem.*, 2018, **266**, 95–105.

8 M. Gosi, A. C. Kumar and Y. Sunandamma, Fluorescence Variation in Selective Sensing of $Hg^{2+}$and Cu^{2+} Ions By Coumarin-xanthene Fused Optical Probe, *J. Fluoresc.*, 2022, **32**, 2379–2393.